HYPERSPECTRAL IMAGING OF SUGAR BEET SYMPTOMS CAUSED BY SOIL-BORNE ORGANISMS

C. Hillnhütter, A.-K. Mahlein, R.A. Sikora, and E.-C. Oerke

Institute of Crop Science and Resource Conservation (INRES), Phytomedicine
Rheinische Friedrich-Wilhelms-Universität Bonn
Nussallee 9, 53115 Bonn, Germany

ABSTRACT

Due to their low mobility, soil-borne pathogens are well suitable for precision agriculture applications. Sensors which assess the reflectance of plant leaves are useful tools to detect and discriminate between soil-borne stressors. In a greenhouse study the symptom development caused by the plant parasitic nematode *Heterodera schachtii* and the fungal pathogen *Rhizoctonia solani* alone or in combination was recorded by means of leaf reflectance with a hyperspectral imaging system twice per week. The sensor recorded in the visible and near infrared (400 – 1000 nm) range. Three image processing methods were tested for their suitability to produce the most sensitive spectral information for disease detection. Nine spectral vegetation indices were calculated from spectra to correlate them to leaf symptoms. The symptoms of *Rhizoctonia* crown and root rot caused by *R. solani* anastomosis group 2-2IIIB and *H. schachtii* could be detected by hyperspectral image analysis. Symptom development in mixed inoculations was faster and more severe than in single inoculations, indicating complex interactions among fungus, nematode and plant. Progress of *Rhizoctonia* crown and root rot could be discriminated for plants attacked by the fungus alone and the combination of both pathogens, respectively. The results from this study under controlled conditions will be used to transfer the sensor technology to the field.

Keywords: *Heterodera schachtii*, *Rhizoctonia solani*, image processing, spectral vegetation indices

INTRODUCTION

The plant parasitic nematode *Heterodera schachtii* (Schmidt) and the soil-borne fungal pathogen *Rhizoctonia solani* (Kühn) [teleomorph *Thanatephorus cucumeris* (Frank) Donk] are two major constraints in sugar beet production worldwide (Schlang, 1991; Kiewnick et al., 2001). Above-ground symptoms

caused by the sugar beet root colonizing nematode are stunted growth, decreased chlorophyll content and wilting of the canopy in the late cropping season due to water stress (Cooke, 1987; Schmitz et al., 2006). *Rhizoctonia* crown and root rot (RCRR) caused by *R. solani* anastomosis group (AG) 2-2IIIB results in yellowing of leaves, which later become necrotic. Furthermore, symptoms include wilting, collapse and formation of a rosette of dying leaves on the soil (Herr, 1996). Both soil-borne organisms appear in patches in the field, have low mobility and induce above-ground symptoms on the canopy, which makes them perfect targets for precision agriculture tools. They in particular include reflectance measurements of plant canopies and mapping of the occurrence of disease symptoms. Several studies have been conducted successfully on the detection of stresses caused by different nematode or soil-borne fungal pathogens on plant canopy reflectance by non-imaging multi- and hyperspectral sensors (Hope et al., 1999; Heath et al., 2000; Nutter et al., 2002; Laudien et al., 2003). Hillnhütter et al. (2009) demonstrated the potential of a non-imaging hyperspectral sensor to assess symptoms caused by *H. schachtii* and *R. solani* on sugar beet plants in greenhouse trials by calculation of spectral vegetation indices (SVIs).

Comparing hyperspectral imaging used in this study to the non-imaging technique used in previous studies, imaging systems have several advantages (Kumar et al., 2001). The spatial resolution of non-imaging sensors is low compared to imaging systems. Non-imaging sensors obtain mixed information of plant material (diseased and not diseased) and soil, whereas the information can be separated using imaging systems (Bravo, 2006). Imaging spectroscopy is the fusion of imaging technology and spectroscopy, in which each pixel of the image is a vector of high resolution spectral information (Noble et al., 2003). Until recently this technology has been used primarily in remote sensing applications, but it has become available now also for near-range hyperspectral imagery and it has been identified as a tool with high potential for disease detection in crop production (Moshou et al., 2006). Symptoms of diseases which are smaller than the leaves may be assessed and analyzed in detail by near-range imaging.

The objective of this study was to examine the potential of near-range hyperspectral imaging to detect and identify stress caused by either *H. schachtii* or *R. solani* alone on sugar beet, or both organisms in combination. Three different methods of image pre-processing were tested to obtain the most sensitive spectral data for detection and discrimination of symptoms caused by the pathogens. In order to detect leaf pathogens by means of reflectance it is important to eliminate the influence of soil reflectance on the spectral information to obtain more sensitive data. A Normalized Difference Vegetation Index (NDVI) threshold is often used to discriminate leaf reflectance from soil reflectance (Moshou et al., 2006). The NDVI was shown to be a good parameter for the discrimination of vegetation from background (Rouse et al., 1974). However, for soil-borne pathogens like *H. schachtii* and *R. solani* soil reflectance may be used for the quantification of disease incidence and plant biomass which decreases with disease severity while the proportion of the soil increases. The influence of soil reflectance on the correlation between SVIs and disease ratings was tested by including or excluding it in pre-processed images. These fundamental steps in image analysis were conducted to identify the optimal processing of images for

further analysis (classification, change detection, etc.) of images and for remotely sensed field data in the future.

MATERIALS & METHODS

Organisms: Sugar beet plants, cultivar Alyssa (susceptible to *H. schachtii* and *R. solani*, KWS GmbH, Einbeck, Germany) were used in this experiment. Seeds were sown in multipots (4.8 × 50 × 28 cm) and grown for 28 days. Plants were grown throughout the experiment at 25/22 °C (day/night), 70 ± 10 % relative humidity and a photoperiod of 12 h d^{-1} (> 300 µmol $m^{-2}s^{-1}$, Phillips SGR 140, Hamburg, Germany) in a greenhouse. After four weeks plants were transplanted into boxes (120 × 80 × 25 cm) containing 240 l substrate with sand; C-horizon; A-horizon and Seramis® (Mars GmbH, Mogendorf, Germany) at a ratio of 2 : 0.6 : 0.4 : 0.4 (v/v). Thirty-two plants were planted into each box with 15 cm spacing between plants within rows and a row width of 20 cm. Each box comprised four rows with eight plants each. Plants were fertilized with 400 g long-term fertilizer Osmocote® Plus (15:9:12, Scotts, Maysville, USA) per box.

Heterodera schachtii was obtained from the institutes' stock cultures. Nematodes were multiplied on *Brassica napus*, cultivar Akela (Feldsaaten Freudenberger, Krefeld, Germany), grown in sand. Cysts were extracted using a standard wet-screen decantation method and were transferred to Oostenbrink dishes filled with 5mM $ZnCl_2$-solution for seven days to stimulate J2 emergence (Oostenbrink, 1960). The J2 larvae were washed on 25 µm sieves (Retsch, Haan, Germany), counted and subsequently used for inoculation of the plants.

Rhizoctonia solani (AG2-2 IIIB) was provided by the Plant Protection Service of North Rhine-Westphalia. A sand-flour protocol developed by Zens et al. (2002) was used for inoculum production; 50 g of sand mixed with 1.5 g wheat flour and 7 ml tap water in a 200 ml Erlenmeyer flask sealed with a paper plug was autoclaved at 121 °C for 50 min. After cooling, the flasks were inoculated with three mycelia pieces (5 mm) of *R. solani* taken from 14 day old cultures grown on PDA (PDB [Becton, Dickinson and Company, Le Pont de Claix, France] + agar [AppliChem, Darmstadt, Germany]). The flasks were incubated at 24 °C in the dark for 14 days and were shaken every second day to optimize fungal growth.

Inoculation: *Rhizoctonia solani* sand-flour inoculum (2.5 g) was placed into 5 cm deep cavities made for the transplantation of seedlings, before transferring the seedlings onto the inoculum into the cavities. The nematode was inoculated into two cavities (3 cm deep) in the soil with a pipette tip near the base of the plant. Each cavity received 1 ml tap water with 1000 J2 of *H. schachtii* (2000 J2/plant).

The experiment included four treatments; untreated control plants; sugar beet inoculated with *H. schachtii* alone; inoculated with *R. solani* alone; inoculated with both organisms in combination. Each treatment consisted of 32 plants. The experiment was conducted twice.

Evaluation of plant and pathogen development: The experiments were terminated nine weeks after inoculation. Fresh weight of beet and shoot were determined for each plant. The percentage of the beet affected by RCRR was rated on a scale of: 0 = healthy, no symptoms, to 6 = beet completely rot, plant dead (Zens et al., 2002). Leaf symptoms induced by *R. solani* were rated according to a protocol of Zens et al. (2002) which classifies wilting, yellowing or

necrosis of leaves on a scale from 0 = plant healthy, no symptoms on petioles, to 6 = leaf brown and necrotic. To determine the number of eggs and juveniles of *H. schachtii*, 100 ml soil-samples were taken with a soil core sampling tool (Oakfield Apparatus Company, Oakfield, USA) where the plants were growing before harvest. The cysts of nematodes were extracted using a wet-screen decantation technique with a sieve combination of 500 µm and 250 µm aperture (Ayoub, 1980). The cysts were transferred to 15 ml homogenization tubes (B. Braun, Melsungen, Germany) in which they were crushed. The number of eggs and J2 per plant was then counted under a stereoscope in a 2 ml RAS-Counting Slide (Hooper et al., 2005) with sloping sides consisting of a 2 mm high plastic ring clued on a plastic plate of 75 × 37 mm, with fortyfold magnification.

Hyperspectral image acquisition and data analysis: Leaf reflectance of plants was recorded starting 5 days after inoculation (dai) to 64 dai twice per week. Hyperspectral images were obtained by a line scanner (ImSpector V10E, Spectral Imaging Ltd., Oulu, Finland) in combination with a mirror scanner, which was mounted under a rack specially constructed for this sensor. Images were recorded in a dark room and the sensor was surrounded by six ASD-Pro-Lamps (Analytical Spectral Devices Inc., Boulder, USA) in order to provide optimum illumination conditions. The ImSpector has a spectral resolution of 2.8 nm and a spectral range from 400 to 1000 nm. After focussing the camera using a black and white test target, the white reference (Spectral Imaging Ltd., Oulu, Finland) and the plants to be recorded were placed in exactly the same position to the camera for each measurement. The images were recorded to the hard disc by the operator software SpectralCube (Spectral Imaging Ltd., Oulu, Finland). Spatial and spectral binning was four and the frame rate and the exposure time had to be optimized. A dark current image was taken by closing the shutter of the camera. Subsequently, the plants were recorded with the white reference and another image, with changed exposure time, without white reference.

The three images - dark current, white reference and raw image - obtained for each treatment were normalized using the program ENVI 4.6 + IDL 7.0 (ITT Visual Information Solutions, Boulder, USA) by a special IDL tool. A normalized image was created by comparing the raw image to the dark current image (minimum) and the white reference (maximum). The Savitzky-Golay smoothing filter (Savitzky and Golay, 1964) obtained from ITT Visual Information Solutions Code Contribution Library was applied to the spectra of the normalized images. The filter was adjusted to the fifth node left and right and a polynomial of third order.

Pre-processed images were used for further analysis. Three approaches were tested for data extraction. In approach 1 the complete image was defined as a region of interest (ROI) and spectral data were extracted from all pixels, plants and soil reflectance. For approach 2, a mask for plant biomass was created by calculating the NDVI (see Tab. 1) of the normalized image to exclude soil reflectance and to extract reflectance data of plant pixels only (NDVI > 0.5). The mask was applied to the normalized image and then a ROI was placed over the image (Fig. 1A; B; C; D). For approach 3, the margins of all leaves per plant were circumscribed manually by polygon-type regions of interest (ROIs); subsequently the mean spectrum of each plant within an image was extracted (Fig. 1E).

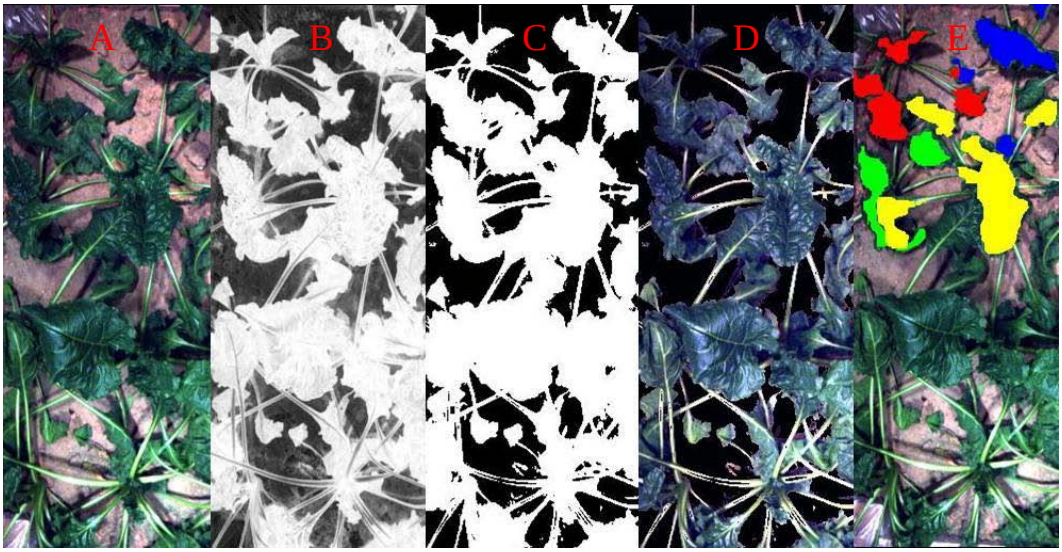

Figure 1: Different stages of processing of images using the program ENVI: A = normalized raw image; B = NDVI transformed normalized raw image for creating a mask; C = mask created from image B; D = mask applied to the normalized raw image A; E = region of interests (ROIs) on leaves.

Different to approach 2, this leaf approach was used to obtain spectral information for the leaves of plants only, excluding petiole and soil reflectance.

For each ROI the mean spectrum was calculated by ENVI and exported as ASCII file. This file was imported to MS Excel 2007 (Microsoft Corporation, Redmond, USA) to calculate nine SVIs of the spectra in a time series (Tab. 1). Spectral vegetation indices from remote sensing were tested for their correlation to ratings of above-ground disease symptoms depending on the method of image processing.

Statistical analysis: The program PASW 18 (SPSS Inc., Chicago, USA) was used for statistical analysis of data. Plant fresh weights were tested for homogeneity of variance and subsequently exposed to analysis of variance (ANOVA). Subgroups were built using Tukey´s test with a probability level of $p < 0.01$. Plant weights were tested on correlation between each other at a probability level of 0.01 by Pearson's correlation coefficient. Correlations between plant weights, leaf symptom rating, RCRR beet rating and NDVI values

Table 1: Spectral vegetation indices used for correlation with leaf symptoms caused by *Rhizoctonia* crown and root rot

Index	Equation	Reference
NDVI	$(R_{800}-R_{670})/(R_{800}+R_{670})$	Rouse et al. (1974)
Carter Index II	R_{695}/R_{760}	Carter et al. (1996)
Lichtenthaler Index I	$(R_{800}-R_{680})/(R_{800}+R_{680})$	Lichtenthaler et al. (1996)
OSAVI	$(1+0.16)\times(R_{800}-R_{670})/(R_{800}+R_{670}+0.16)$	Rondeaux et al. (1996)
mCAI	$(R_{545}+R_{752})/2\times(752–545)–\Sigma(R\times2.8)$	Laudien et al. (2003)
NDI	$(R_{750}-R_{705})/(R_{750}+R_{705})$	Gitelson et al. (1994)
SRPI	R_{430}/R_{680}	Penuelas et al. (1995)
PWI	R_{970}/R_{900}	Penuelas et al. (1997)
PRI	$(R_{550}-R_{531})/(R_{550}+R_{531})$	Gamon et al. (1992)

were also calculated. Nine SVIs were correlated to leaf symptom ratings (Zens et al., 2002) using Spearman's rank correlation coefficient. The RCRR beet rating and the number of eggs and J2 per plant were compared using the t-test ($p < 0.05$).

RESULTS

Plant and pathogen development: No differences were detected in plant development and leaf reflectance among treatments until 28 dai. Symptoms were not visible, neither from *H. schachtii* nor from *R. solani*. Symptoms of leaf wilting became visible on *H. schachtii* inoculated plants from 28 dai to 40 dai. Wilted leaves were detected predominantly for plants inoculated with *H. schachtii* alone. These observations were in accordance with the higher number of eggs and larvae in boxes inoculated with *H. schachtii* only compared to the combined inoculation (Tab. 2).

Forty days after inoculation first leaf symptoms caused by RCRR became visible at the petioles of the oldest leaves (Fig. 2). These symptoms were not visible until 50 dai and 54 dai in the closed canopy of plants inoculated with the combination of *H. schachtii* and *R. solani* and with *R. solani* alone, respectively. Leaf symptom ratings showed significant differences between the *R. solani* inoculated treatments starting 47 dai (Fig. 2).

Table 2: Influence of *Heterodera schachtii* and *Rhizoctonia solani* alone or in combination on the number of J2 larvae and eggs of *H. schachtii* and *Rhizoctonia* crown and root rot (RCRR) beet rating. Columns with different letters indicate significant difference (t-test, $p < 0.05$, $n = 16$)

Treatment	Number of eggs and J2	RCRR beet rating
Heterodera schachtii	12,375 ± 408b	-
Rhizoctonia solani	-	2.97 ± 0.31a
H. schachtii + *R. solani*	5,987 ± 257a	5.13 ± 0.27b

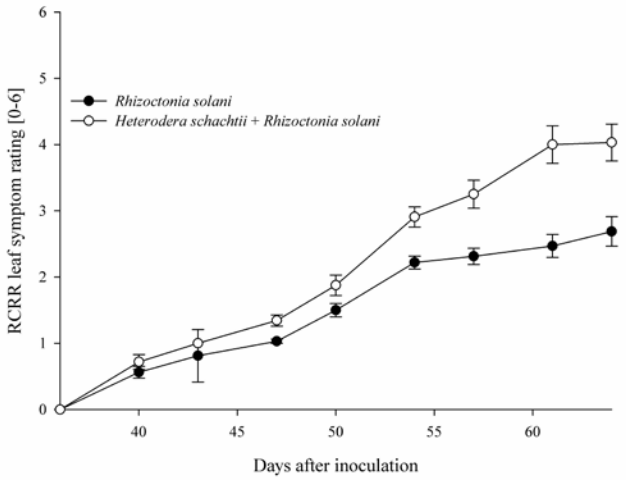

Figure 2: Effect of *Rhizoctonia solani* alone and in combination with *Heterodera schachtii* on the development of sugar beet leaf symptoms. Bars indicate standard error of the mean ($n = 32$).

The number of eggs and larvae of *H. schachtii* was significantly higher in the treatment with the nematode alone compared to the mixed inoculation. *Vice versa* beet rot was significantly more severe in the mixed inoculation compared to plants inoculated with *R. solani* alone (Tab. 2).

Fresh weights of leaves and beets clearly indicated an interaction between the two pathogens on sugar beet. Leaves and beets of plants inoculated with the combination of *R. solani* and *H. schachtii* had the lowest biomass of all treatments (Fig. 3). Leaf weights were correlated to beet weights ($r = 0.83$, $p < 0.01$).

Near-range sensing of sugar beet crops: Three different methods of image processing were tested to monitor symptom development caused by *H. schachtii* and *R. solani*, respectively. Subsequently, nine SVIs were tested on their correlation to leaf symptoms in dependence to the pre-processing methods.

The different approaches of image processing influenced the accuracy to monitor leaf symptom development caused by the soil-borne pathogens. Plants inoculated with *H. schachtii* showed leaf wilting from 28 dai to 40 dai, resulting in lower NDVI values. Forty dai the plants recovered from wilting (Fig. 4 A). These wilting symptoms caused by *H. schachtii* were best shown by NDVI obtained with the first processing approach including soil reflectance. In contrast, methods excluding soil reflectance resulted in only marginal changes of NDVI. Starting 50 dai, the NDVI of sugar beet inoculated with both pathogens was decreased. This was shown by all processing approaches (Fig. 4 A; B; C). Using approach 1, the NDVI of a canopy of non-inoculated plants was significantly higher than that of sugar beet inoculated with *R. solani* alone 64 dai and later (Fig. 4 A). Image processing approach 3 - use of leaf pixels only - however, resulted in the discrimination between these treatments already 7 days earlier (Fig. 4 C). Approach 2 - exclusion of soil reflectance - was less sensitive in the discrimination of leaf symptoms caused by the pathogens (Fig. 4 B).

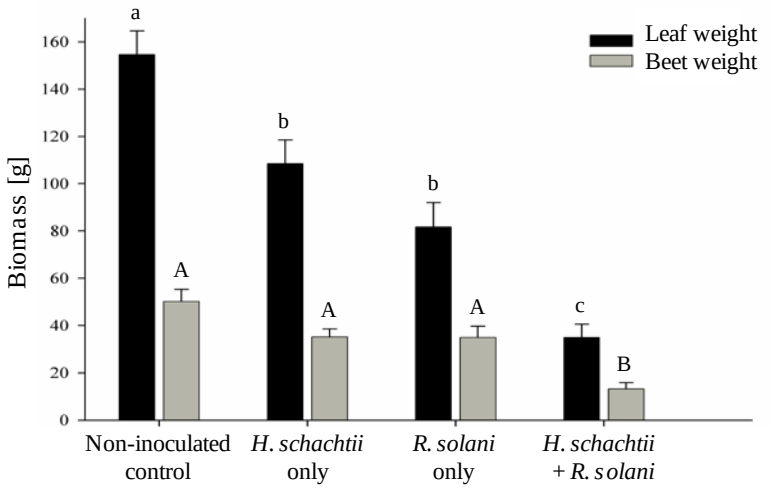

Figure 3: Mean leaf and beet weight of sugar beet plants inoculated with either *Heterodera schachtii* or *Rhizoctonia solani* alone or with the combination of both pathogens. Error bars represent the standard error of the mean. Different letters indicate significant difference among treatments according to Tukey's test ($p < 0.01$, $n = 32$).

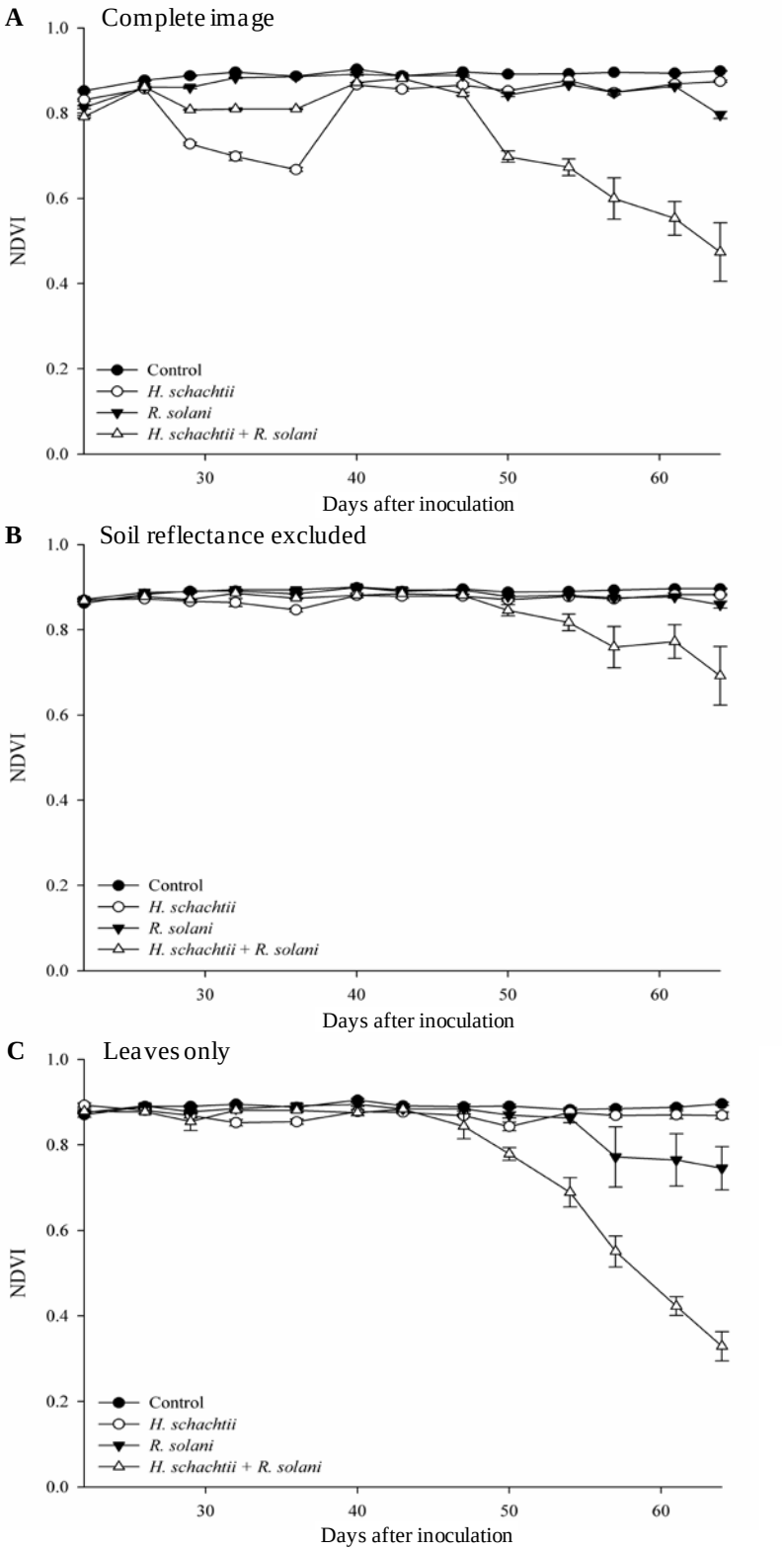

Figure 4: Influence of image processing on NDVI calculated from spectra of sugar beet inoculated with either *Heterodera schachtii* or *Rhizoctonia solani* alone or with the combination of both pathogens

The leaf weight of sugar beet plants was correlated to the NDVI calculated from approach 1 (r = 0.6, p < 0.01). Furthermore, as leaf symptom ratings were related to RCRR beet rot ratings (r = 0.93, p < 0.01), the NDVI was also correlated to RCRR beet rating (r = -0.84, p < 0.01).

The nine SVIs calculated from canopy spectra considerably differed in their correlation to leaf symptoms of sugar beet plants depending on the three image processing approaches. Processing approach 1 which included soil reflectance resulted by far in the highest correlation between leaf symptom rating and NDVI (Tab. 3). Approach 2 - exclusion of soil - gave the highest correlations of pigment-specific SVIs to leaf symptom ratings. Especially indices related to photosynthesis (PRI, Lichtenthaler Index I, SRPI) gave the best correlations to visual symptom ratings (r = -0.85 to -0.88). In contrast, NDVI and PWI had the lowest correlation coefficients when using image processing approach 2. The plant water index (PWI) was the only SVI which showed a significantly better correlation to leaf symptom ratings when applying image processing approach 3; however, with r = 0.32 the correlation was statistically not significant (Tab. 3).

DISCUSSION

Nematode-inoculated plants started to wilt after completion of the first generation cycle of *H. schachtii* due to the penetration of the second generation into the roots. The developmental stage of nematodes was calculated by the heat sum-model according to Čuri and Zmoray (1966) which confirmed the time of initiation of first symptoms. After a heat sum of 465 °C (32 dai) first wilting symptoms of leaves were detected. The plants recovered after about ten days by the production of secondary roots which leads to a reduction of leaf and beet masses (Cooke, 1987). However, plants inoculated with *H. schachtii* alone showed more severe wilting than the *R. solani* and *H. schachtii* together inoculated plants. The activity of *R. solani* is likely to inhibit the development of *H. schachtii* due to rotting of the potential habitat of the nematode which is an obligate biotrophic pathogen.

In the presence of the nematode the development of RCRR was faster and more severe as compared to sugar beets attacked by *R. solani* alone. The fungal pathogen may be able to use the penetration sites of *H. schachtii* to enter the

Table 3: Spearman's correlation coefficient for the relation between leaf symptoms caused by *Rhizoctonia* crown and root rot and nine vegetation indices depending on the pre-processing method for hyperspectral images from sugar beet plants (p < 0.01; n = 128).

Index	Image processing approach		
	Complete image	Soil excluded	Leaves only
NDVI	-0.93	-0.69	-0.74
Carter Index II	0.73	0.71	0.73
Lichtenthaler Index I	-0.71	-0.86	-0.74
OSAVI	-0.73	-0.82	-0.69
mCAI	-0.71	-0.79	-0.65
NDI	-0.73	-0.80	-0.67
SRPI	-0.62	-0.85	-0.74
PWI	0.34	0.09	0.32
PRI	-0.71	-0.88	-0.78

plants (Bergeson, 1972). This leads to the conclusion that *H. schachtii* promotes the development of the fungal pathogen, whereas the fungus inhibited the development of the cyst nematode.

The significant correlation between biomass of leaves and beets demonstrated the importance of leaves as the source of assimilates for beet development. This close relationship between leaves and beets is the basis for the large potential of NDVI measurements for assessment of below-ground damage of plants due to pathogens. Non-destructive hyperspectral near-range sensing may be used in time series experiments on host-pathogen interactions as well as in screening systems for crop resistance to pests attacking and damaging the root system of crops.

Three approaches of image processing were tested for their usefulness to assess the development of sugar beet symptoms due to *H. schachtii* and *R. solani.* The NDVI confirmed to be a very good indicator of ground cover and biomass of plants as reported by Rouse et al. (1974). Sensitivity was suitable to detect the damage due to penetration of the second generation of *H. schachtii* larvae as well as the transient recovery of plants. Since wilted leaves did not cover the soil as leaves of healthy plants did, increased soil reflectance decreased NDVI when the complete image was analyzed. This approach was similar to a non-imaging approach resulting in a spectral mixing of reflectance from crop and soil. In contrast, image processing approaches leading to pure plant reflectance resulted in only marginal changes of NDVI despite of considerable leaf wilting. The NDVI was not suitable to assess the water status of plant tissue. Spectral vegetation indices sensitive to drought stress, therefore, should be tested for the detection of spectral differences between nematode-inoculated and control plants.

Above-ground symptoms of RCRR are mainly yellowing of sugar beet leaves and the formation of a rosette of dying leaves on the soil in later stages (Herr, 1997). Leaf symptoms were closely correlated to NDVI obtained from images including soil reflectance, whereas image processing approaches eliminating the soil gave considerable weaker correlations. This indicates that NDVI is highly sensitive to changes in soil cover from crops. However, it seems not to be suitable for the detection of disease-specific modifications of plant tissue. Pure plant pixel approaches were not very suitable for the assessment of crop biomass.

The other SVIs tested are mainly pigment specific (Lichtenthaler Index I, Carter II, mCAI, NDI, OSAVI, PRI, SRPI) or give information on the water status of plants (PWI). They are commonly used in remote sensing, but - similar to NDVI - largely lack specificity for the detection of plant diseases. Nevertheless, the second approach with elimination of soil reflectance significantly increased their correlation to leaf symptom ratings. This approach was used by Moshou et al. (2006) in order to remove soil reflectance for the discrimination of yellow rust from nutrient stress of wheat leaves. For sugar beet, the PRI had the highest correlation to leaf symptoms. It has been developed for tracking of photosynthetic light use efficiency (Gamon et al., 1992). The PRI proved to be more precise in the detection of physiological changes in leaves resulting from disease development than the NDVI as also stated by Gamon et al. (1992). Also the Lichtenthaler Index I which was developed for the assessment of leaf fluorescence (Lichtenthaler et al., 1996) and the SRPI related to carotenoid and chlorophyll a content of plant tissue (Penuelas et al., 1995) showed higher correlations to leaf symptoms.

The extraction of reflectance data by leaf-specific ROIs gave the weakest correlations between SVIs and leaf symptoms incited by RCRR. This method was used for the assessment of leaf photosynthesis (Rascher et al., 2007). These authors discussed its usefulness because of the manual selection of leaf area by ROIs and the non-normal distribution of data. Furthermore, the manual selection is more time consuming than the use of a mask based on NDVI threshold values. Correlations between leaf symptoms and NDVI, Carter Index and PWI were better in the third approach than in the second. This may be due to omitting the beet crown and petioles in ROIs. In addition, dead leaves selected by ROIs had spectral properties similar to the soil and contributed to the assessment of necrotic plant tissue as a leaf symptom of RCRR.

The use of unprocessed images allowed the assessment of differences in plant biomass as measured by NDVI. The elimination of pixels representing the soil or non-relevant plant tissue gave the possibility to use pigment-specific SVIs for the detection of physiological changes in plant tissue due to the development of root diseases. Therefore, leaf symptoms caused by either *R. solani* or *H. schachtii* have to be investigated more in detail on the tissue level. Disease-specific SVIs and/or combinations of SVIs may be applied in hyperspectral imaging of plant diseases in order to achieve improved correlations and early detection of symptoms. In further image analysis, supervised classification tests (e.g. spectral angle mapper; minimum distance; maximum likelihood) known from remote sensing will be tested also on the detection of disease symptoms.

ACKGNOWLEDGEMENTS

The authors gratefully acknowledge financial, educational and logistical support from Research Training Group 722 ‘Information Techniques for Precision Crop Protection’, funded by the German Research Foundation (DFG). The companies KWS and Feldsaaten Freudenberger are thanked for providing seed material. We are also thankful for the development of the IDL tool for normalization of hyperspectral images by Dr. Albert Moll.

REFERENCES

Ayoub, S.M. 1980. Plant Nematology – an agricultural training aid. NemaÁid Publication, Sacramento, USA, 195pp.

Bergeson, B.B. 1972. Concepts of nematode-fungus associations in plant disease complexes: A review. Exp Parasitol 32, 301-314.

Bravo, C. 2006. Automatic foliar disease detection in winter wheat. PhD Thesis University Leuven, 258p.

Carter, G.A., Dell, T.R. and Cibula, W.G. 1996. Spectral reflectance characteristics and digital imagery of a pine needle blight in the southern United States. Can J For Res 26, 402-407.

Cooke, D.A. 1987. Beet cyst nematode (*Heterodera schachtii* Schmidt) and its control on sugar beet. Agr Zool Rev 2, 135-183.

Čuri, J. and Zmoray, I. 1966. The relation of climatic factors to the duration of the development of *Heterodera schachtii* in Slovakia (ČSSR). Helminthologica 7, 49-63.

Gamon, J.A., Penuelas, J. and Field, C.B. 1992. A narrow-waveband spectral index that tracks diurnal changes in photosynthetic efficiency. Int J Remote Sens 41, 35-44.

Gittelson, A.A. and Merzlyak, M.N. 1994. Spectral reflectance changes associated with autumn senescence of *Aesculus hippocastanum* L. and *Acer platanoides* L. leaves. Spectral features and relation to chlorophyll estimation. J Plant Physiol 143, 286-292.

Heath, W.L., Haydock, P.P.J., Wilcox, A. and Evans, K. 2000. The potential use of spectral reflectance from the potato crop for remote sensing of infection by potato cyst nematodes. Aspect Appl Biol 60, 185-188.

Herr, L.J. 1996. Sugar beet diseases incited by *Rhizoctonia* species. (p. 341-349). *In: Sneh, B., Jabaji-Hare, S., Neate, S. and Dijst, G. (Eds).* Rhizoctonia *species: Taxonomy, Molecular Biology, Ecology, Pathology and Disease Control.* Kluwer Academic Publishers, Dordrecht, Netherlands.

Hillnhütter, C., Sikora, R.A. and Oerke, E-.C. 2009. Detection of complex soil-borne disease interactions by hyperspectral foliar surface monitoring in sugar beet. Phytopathology 99, 53.

Hooper, D.J., Hallmann, J. and Subbotin, S. 2005. Methods for extraction, processing and detection of plant and soil nematodes. (p 53-86). *In: Luc, M., Sikora, R.A. and Bridge, J. (Eds.) Plant Parasitic Nematodes in Subtropical and Tropical Agriculture.* CABI Publishing, Wallingford, UK.

Hope, A., Coulter, L., Stow, D., Peterson, S., Service, D., Telk, A. and Melin, D. 1999. Root rot detection in sugar beet using digital multispectral video. *Proceedings AARS, 20th Asian Conference on Remote Sensing*, November 22-25, 1999, Hong Kong, China.

Kiewnick, S., Jacobsen, B.J., Braun-Kiewnick, A., Eckhoff, J.L.A. and Bergman, J.W. 2001. Integrated control of *Rhizoctonia* crown and root rot of sugar beet with fungicides and antagonistic bacteria. Plant Dis 85, 718-722.

Kumar, L., Schmidt, K. S., Dury, S., and Skidmore, A. K. 2001. Imaging spectrometry and vegetation science. (p. 111-155). *In: van der Meer, F., and de Jong, S. M. (Eds). Imaging spectrometry.* Kluwer Academic Publishers, Dordrecht, Netherlands.

Laudien, R.K., Bareth, G. and Doluschitz, R. 2003. Analysis of hyperspectral field data for detection of sugar beet diseases. *Proceedings of the EFITA Conference*, July 5-9, 2003, Debrecen, Hungary.

Lichtenthaler, H.K., Lang, M., Sowinska, M., Heisel, F. and Miehe, J.A. 1995. Detection of vegetation stress via a new high resolution fluorescence imaging system. J Plant Physiol 148, 599-612.

Moshou, D., Bravo, C., Wahlen, S., West, J., McCartney, A., de Baerdemaeker, J. and Ramon, H. 2006. Simultaneous identification of plant stresses and diseases in arable crops using proximal optical sensing and self-organizing maps. Precis Agric 7, 149-164.

Noble, S.D., Crookshank, M. and Crowe, T.G. 2003. The design of a ground-based hyperspectral imaging / imaging spectrophotometer system. *Proceedings of the CSAE/SCGR Conference*, July 6-9, 2003, Montreal, Canada.

Nutter, F.W., Tylka, G.L., Guan, J., Moreira, A.J.D., Marett, C.C., Rosburg, T.R., Basart, J.P. and Chong, C.S. 2002. Use of remote sensing to detect soybean cyst nematode-induced plant stress. J Nematol 34, 222-231.

Oostenbrink, M. 1960. Estimating nematode populations by some selected methods. (p. 85-102). *In: Sasser, J.N. & Jenkins, W.R. (Eds). Nematology*. University of North Carolina Press, Chapel Hill, USA.

Peñuelas, J., Filella, I., Lloret, P., Munoz, F. and Vilajeliu, M. 1995. Reflectance assessment of mite effects on apple trees. Int J Remote Sens 16, 2727-2733.

Peñuelas, J., Pinol, J., Ogaya, R. and Filella, I. 1997. Estimation of plant water concentration by the reflectance water index WI (R900/R970). Int J Remote Sens 18, 2869-2875.

Rascher, U., Nichol, C.J., Small, C. and Hendricks, L. 2007. Monitoring spatio-temporal dynamics of photosynthesis with a portable hyperspectral imaging system. Photogramm Eng Rem S 73, 45-56.

Rondeaux, G., Steven, M. and Baret, F. 1996. Optimization of soil-adjusted vegetation indices. Int J Remote Sens 55, 95-107.

Rouse, J.W., Haas, R.H., Schell, J.A., Deering, D.W. and Harlan, J.C. 1974. Monitoring the vernal advancements and retrogradiation of natural vegetation. *Proceedings of the 3rd Earth Resources Technology Satellite-1 Symposium*. December 10-14, 1973, Washington D.C., USA.

Savitzky, A. and Golay, M.J.E. 1964. Smoothing and differentiation of data by simplified least squares procedures. Anal Chem 36, 1627-1639.

Schlang, J. 1991. Anbau resistenter Zwischenfrüchte zur biologischen Bekämpfung des Rübenzystennematoden. Zuckerrübe 40, 476-488.

Schmitz, A., Tartachnyk, I.I., Kiewnick, S., Sikora, R.A. and Kühbauch, W. 2006. Detection of *Heterodera schachtii* infestation in sugar beet by means of laser-induced and pulse amplitude modulated chlorophyll fluorescence. Nematology 8, 273-286.

Zens, I., Steiner, U. and Dehne, H.-W. 2002. Auftreten, Charakterisierung und Kontrolle des Erregers der Rübenfäule, *Rhizoctonia solani*, in Nordrhein-Westfalen. *Landwirtschaftliche Fakultät der Universität Bonn, Schriftenreihe des Lehr- und Forschungsschwerpunktes USL* 91, 99 p.